photochem

MDPI

Article

[2+2]-Photocycloadditions of 2-Acetoxy-1,4-naphthoquinone and Structure Determination of the Main Photoadducts

Madyan A. Yaseen [1,2], Zhifang Guo [1], Peter C. Junk [1] and Michael Oelgemöller [1,3,*]

[1] College of Science and Engineering, James Cook University, Townsville, QLD 4811, Australia; madyan.yaseen@uosamarra.edu.iq (M.A.Y.)
[2] College of Education, University of Samarra, Samarra 34010, Iraq
[3] Faculty of Chemistry and Biology, Hochschule Fresenius gGmbH—University of Applied Sciences, 65510 Idstein, Germany
* Correspondence: michael.oelgemoeller@jcu.edu.au

Abstract

The [2+2]-photocycloaddition of 2-acetoxy-1,4-naphthoquinone with 1,1-diphenylethylene, styrene and cyclopentene was conducted in a conventional batch reactor. Prolonged irradiation selectively produced the corresponding *anti* and *head-to-head* cyclobutanes in acceptable to good yields. The batch process was subsequently transferred to continuous-flow operation in a simple capillary device. Likewise, the photocycloaddition with diphenylacetylene gave the corresponding cyclobutene and a benzoanthracenone derivative in acceptable yields. The crystal structures of all main photoproducts were successfully determined.

Keywords: photocycloaddition; 2-acetoxy-1,4-naphthoquinone; cyclobutane; cyclobutene; continuous flow-photochemistry

Academic Editor: Diego Sampedro

Received: 1 September 2025
Revised: 30 September 2025
Accepted: 1 October 2025
Published: 10 October 2025

Citation: Yaseen, M.A.; Guo, Z.; Junk, P.C.; Oelgemöller, M. [2+2]-Photocycloadditions of 2-Acetoxy-1,4-naphthoquinone and Structure Determination of the Main Photoadducts. *Photochem* **2025**, *5*, 31. https://doi.org/10.3390/photochem5040031

1. Introduction

1,4-naphthoquinone derivatives play an important role as biologically active natural products in medicinal chemistry and building blocks in organic synthesis [1–5]. The spectroscopic properties and photochemistry of 1,4-naphthoquinones have been likewise widely explored [6–9]. The [2+2]-photocycloaddition has been studied in particular [10,11], and selected photoadducts have shown promising biological activities [12,13]. In general, 2-substituted 1,4-naphthoquinones can form a variety of regio- (head-to-head vs. head-to-tail) and diastereoisomeric (syn vs. anti) cyclobutanes (Scheme 1).

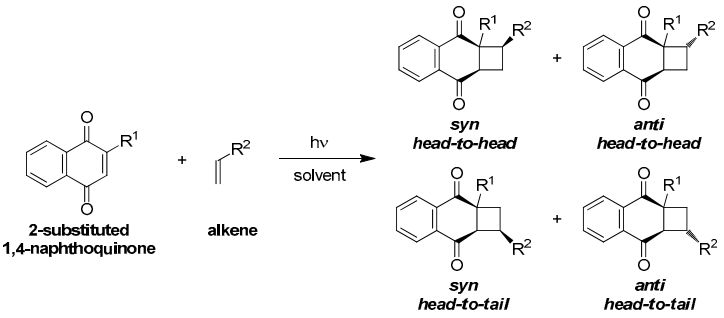

Scheme 1. [2+2]-Photocycloadditions of 2-substituted 1,4-naphthoquinones with alkenes to diastereo- and regioisomeric cyclobutanes.

Traditionally, photochemical transformations are performed under batch conditions using medium-pressure mercury lamps and hazardous solvents [14,15]. The inhomoge-

neous light distribution and limited mass-transfer within these devices often necessitate exhaustive irradiations that favor photodecomposition and reduce product yields and purities [16]. To overcome these limitations, photochemical transformations are now routinely conducted under continuous-flow conditions [17–22]. Thus far, flow-photochemical transformations of quinones are rare and have predominantly focused on the parent, unsubstituted 1,4-naphthoquinone [23–26]. As part of a PhD study [27], this work investigates [2+2]-photocycloadditions of 2-acetoxy-1,4-naphthoquinone (**1**) as a model compound [28–30].

2. Materials and Methods

2.1. General Information

All starting materials, reagents and solvents were purchased from commercial suppliers (Merck Life Science Pty Ltd., Bayswater, VIC, Australia, or Thermo Fisher Scientific Australia Pty Ltd., Scoresby, VIC, Australia) and were used as received.

Batch irradiations were performed in a Rayonet RPR-200 photochemical chamber reactor (Southern New England Ultraviolet Company, Branford, CT, USA) carrying 16 × 8 W UVB (306 ± 20 nm, G8T5E, Ushio Inc., Tokyo, Japan), UVA (352 ± 20 nm, F4T5BL, Ushio Inc., Tokyo, Japan) or visible light (419 ± 25 nm, RPR-4190A, Southern New England Ultraviolet Company, Brandford, USA) fluorescent tubes. Schlenk flasks equipped with a cold finger and made from Pyrex glass ($\lambda \geq 300$ nm) were used as reaction vessels (capacity: approx. 60 mL). Photoreactions were monitored by thin-layer chromatography (TLC). Continuous-flow operations were conducted using a previously described in-house reactor module equipped with a single 8 W UVA (352 ± 20 nm, F4T5BL, Ushio Inc., Tokyo, Japan) fluorescent tube [31]. Additional technical information and pictures of the reactors can be found in the Supplementary Materials.

Thin-layer chromatography was completed in glass jars on silica gel plates (polygram sil G UV_{254}, Macherey-Nagel GmbH & Co KG, Düren, Germany) and using a 1:4 (vol%) mixture of ethyl acetate and *n*-hexane as the mobile phase. A CombiFlash® Rf+ Lumen™ flash chromatography system (Teledyne Isco, Lincoln, NE, USA) was utilized for product purification. Normal phase cartridges were used as stationery, and a 1:4 (vol%) mixture of ethyl acetate and *n*-hexane as the mobile phase.

Melting points were measured in open capillaries using a Tathastu or Gallenkamp melting point apparatus and were uncorrected.

Nuclear magnetic resonance (NMR) spectroscopy was conducted on a Bruker 400 Ascend™ (^{1}H: 400 MHz and ^{13}C: 100 MHz) equipped with an auto-sampler. Spectra were generated with the MestReNova software (Version 6.0.2-5475, Mestrelab Research S.L., Santiago de Compostela, Spain) using the residual solvent peak as reference. Samples were prepared in $CDCl_3$ (δ = 7.26/77.3 ppm) [32]. The NMR spectra of all photocycloaddition products can be found in the Supplementary Materials.

Mass spectra were recorded using direct injection on a Shimadzu LCMS-2020 equipped with a DUIS ion source. Ions were subsequently detected in positive and/or negative mode within a mass range of m/z 100–500. The mobile phases were aqueous solutions of HPLC-grade methanol or acetonitrile with 0.1% formic acid added. All experimental event sequences were controlled, and processing was performed using LabSolutions for LCMS-2020 software.

Infrared spectra were recorded on a Perkin Elmer Spectrum One FT-IR Spectrometer as thin films. Spectra were recorded in the range of 600–4000 cm^{-1}.

Structure determinations were conducted on the MX1 beamline at the Australian Synchrotron [33]. Crystallographic data (excluding structure factors) for the structures in this paper have been deposited with the Cambridge Crystallographic Data Centre (CCDC)

as supplementary numbers CCDC2345860 (**3a**), CCDC2345861 (*anti*-**3b**), CCDC2345862 (*anti*-**3c**) and CCDC2345863 (**6**), respectively. The data files can be obtained free of charge from the CCDC.

2.2. General Procedure for Photocycloadditions Under Batch Conditions

A solution of 2-acetoxy-1,4-naphthoquinone (1 mmol) and alkene or alkyne (5 mmol) in the respected organic solvent (50 mL) was irradiated in a Schlenk flask for 10–20 h while being purged with a slow stream of nitrogen gas. The reaction mixture was evaporated to dryness, and the residue was subjected to automated column chromatography.

2.3. General Procedure for Photocycloadditions Under Continuous-Flow Conditions

The capillary of the continuous-flow reactor was filled with acetone, and the cooling fans and fluorescent tube were started. A solution of 2-acetoxy-1,4-naphthoquinone (0.5 mmol) and alkene or alkyne (2.5 mmol) in acetone (25 mL) was degassed with nitrogen for 5 min, drawn into a glass syringe and pumped through the in-house flow photoreactor. At the end of the delivery, the capillary was flushed with approx. 15 mL of acetone. The reaction mixture and solvent washings were collected in an amber round-bottom flask. The products were isolated as described above.

2.4. Spectroscopic Details

Compound **1** and photoadducts **3a**, **3b** and **6** are known, and their spectroscopic data matched previously described data [28,29,34,35].

2-Acetoxy-l,4-naphthoquinone (**1**) [34]. Yellowish prisms. M.p.: 124–126 °C (Lit. 131–132 °C). ^{1}H-NMR (400 MHz, $CDCl_3$): δ (ppm) = 2.39 (s, 3H, CH_3), 6.76 (s, 1H, CH_{quin}), 7.78 (m, 2H, CH_{arom}), 8.12 (m, 2H, CH_{arom}). ^{13}C-NMR (100 MHz, $CDCl_3$): δ (ppm) = 20.9, 126.3, 126.8, 127.3, 131.3, 132.2, 134.3, 134.7, 154.6, 167.7, 178.9, 184.8.

3,8-Dioxo-2,2-diphenyl-1,2,2a,3,8,8a-hexahydrocyclobuta[*b*]naphthalen-2a-yl acetate (**3a**) [29]. Colorless solid. M.p.: 192–193 °C (Lit. 191–192 °C). ^{1}H-NMR (400 MHz, $CDCl_3$): δ (ppm) = 2.08 (s, 3H, CH_3), 3.46 (ddd, *J* = 12.3, 7.6 Hz, 2H, CH_2), 3.57 (dd, *J* = 10.6, 4.6 Hz, 1H, CH), 6.88 (dd, *J* = 6.8 Hz, 1H, CH_{arom}), 6.99 (dd, *J* = 7.7 Hz, 2H, CH_{arom}), 7.22 (dd, *J* = 7.4, 1.3 Hz, 3H, CH_{arom}), 7.34 (dd, *J* = 7.7 Hz, 2H, CH_{arom}), 7.49 (dd, *J* = 8.4, 1.2 Hz, 2H, CH_{arom}), 7.53 (dd, *J* = 7.6, 1.5 Hz, 1H, CH_{arom}), 7.58 (ddd, *J* = 7.5, 1.5 Hz, 1H, CH_{arom}), 7.79 (dd, *J* = 7.4, 1.3 Hz, 1H, CH_{arom}), 7.94 (dd, *J* = 7.8, 1.7 Hz, 1H, CH_{arom}). ^{13}C-NMR (100 MHz, $CDCl_3$): δ (ppm) = 20.9, 34.0, 49.1, 58.7, 85.5, 126.6, 126.8, 127.1, 127.3, 127.6, 128.1, 128.2, 128.3, 133.9, 134.0, 134.9, 135.3, 139.6, 143.8, 170.5, 192.5, 196.0. MS (DUIS): *m*/*z* = 397 [M^+ + H], expected: 396 [M^+]. IR (neat): ῡ (cm^{-1}) = 1723, 1687, 1593, 1293, 1276, 1217, 1085, 784.

3,8-Dioxo-2-phenyl-1,2,2a,3,8,8a-hexahydrocyclobuta[*b*]naphthalen-2a-yl acetate (*anti*-**3b**) [29]. Colorless crystals. M.p.: 147–148 °C (Lit. 134–136 °C). ^{1}H-NMR (400 MHz, $CDCl_3$): δ (ppm) = 2.00 (s, 3H, CH_3), 2.59 (ddd, *J* = 12.1, 9.3, 4.6 Hz, 1H, CH), 3.11 (ddd, *J* = 12.0, 11.1, 9.1 Hz, 1H, CH), 3.62 (ddd, *J* = 11.1, 4.6, 1.2 Hz, 1H, CH), 3.98 (dd, *J* = 9.1 Hz, 1H, CH), 7.27–7.33 (m, 3H, CH_{arom}), 7.34–7.41 (m, 2H, CH_{arom}), 7.84 (dd, *J* = 5.8, 3.3 Hz, 2H, CH_{arom}), 8.21 (dd, *J* = 6.2, 3.3 Hz, 1H, CH_{arom}), 8.28 (dd, *J* = 5.9, 2.9 Hz, 1H, CH_{arom}). ^{13}C-NMR (100 MHz, $CDCl_3$): δ (ppm) = 20.6, 28.2, 45.6, 49.7, 81.2, 127.5, 127.8, 128.3, 128.5, 133.7, 134.7, 134.8, 135.0, 136.1, 170.5, 192.0, 195.9. MS (DUIS): *m*/*z* = 321 [M^+ + H], expected: 320 [M^+]. IR (neat): ῡ (cm^{-1}) = 1725, 1687, 1593, 1268, 1214, 1122, 971.

4,9-Dioxo-2,3,3a,3b,4,9,9a,9b-octahydro-1*H*-cyclopenta [3,4]cyclobuta[1,2-*b*]naphthalen-3b-yl acetate (*anti*-**3c**). Colorless crystals. M.p.: 183–184 °C. ^{1}H-NMR (400 MHz, $CDCl_3$): δ (ppm) = 1.51–1.75 (m, 2H, CH_2), 1.78–2.01 (m, 3H, CH), 2.11 (s, 3H, CH_3), 2.38 (dd, *J* = 13.8, 6.1 Hz, 1H, CH), 2.70 (dd, *J* = 12.9, 6.3 Hz, 1H, CH), 2.90 (t, *J* = 8.0 Hz, 1H, CH), 3.03 (d, *J* = 6.9 Hz, 1H, CH), 7.73–7.83 (m, 2H, CH_{arom}), 8.08–8.12 (m, 1H, CH_{arom}), 8.14–8.19 (m, 1H,

CH_{arom}). ^{13}C-NMR (100 MHz, $CDCl_3$): δ (ppm) = 20.3, 25.5, 26.8, 32.9, 40.2, 43.8, 56.2, 75.7, 127.6, 127.9, 133.4, 133.9, 134.6, 134.8, 170.2, 194.2, 194.3. MS (DUIS): m/z = 285 [M^+ + H], expected: 284 [M^+]. IR (neat): ῡ (cm^{-1}) = 1730, 1686, 1592, 1243, 1227, 1062, 997.

3,8-Dioxo-1,2-diphenyl-2a,3,8,8a-tetrahydrocyclobuta[*b*]naphthalen-2a-yl acetate (**6**) [35]. Yellowish crystals. M.p.: 211–212 °C (Lit. 209–211 °C). ^{1}H-NMR (400 MHz, $CDCl_3$): δ (ppm) = 2.22 (s, 3H, CH_3), 4.34 (s, 1H, =CH), 7.37–7.30 (m, 6H, CH_{arom}), 7.60–7.55 (m, 2H, CH_{arom}), 7.73–7.66 (m, 4H, CH_{arom}), 7.96–7.92 (m, 1H, CH_{arom}), 8.14–8.09 (m, 1H, CH_{arom}). ^{13}C-NMR (100 MHz, $CDCl_3$): δ (ppm) = 20.7, 60.2, 80.6, 127.5, 127.6, 127.7, 128.3, 128.7, 128.8, 129.5, 130.1, 131.3, 132.1, 132.9, 133.6, 134.4, 134.8, 137.9, 144.0, 171.0, 192.3, 194.3. MS (DUIS): m/z = 394 [M^+], expected: 394 [M^+]. IR (neat): ῡ (cm^{-1}) = 1728, 1682, 1584, 1444, 1278, 1265, 1228, 1138, 1055, 902, 762.

7-Benzoyl-4-oxo-4*H*-benzo[*de*]anthracen-5-yl-acetate (**7**). Yellow solid. M.p.: 196–197 °C. ^{1}H-NMR (400 MHz, $CDCl_3$): δ (ppm) = 2.32 (s, 3H, CH_3), 7.35 (s, 1H, =CH), 7.48 (dd, J = 7.9 Hz, 2H, CH_{arom}), 7.57 (dd, J = 7.5 Hz, 1H, CH_{arom}), 7.65 (dd, J = 7.7 Hz, 1H, CH_{arom}), 7.69 (d, J = 8.0 Hz, 1H, CH_{arom}), 7.79 (dd, J = 8.3 Hz, 1H, CH_{arom}), 7.91 (d, J = 8.0 Hz, 2H, CH_{arom}), 8.00 (dd, J = 8.0 Hz, 1H, CH_{arom}), 8.74 (d, J = 8.6 Hz, 1H, CH_{arom}), 8.80 (d, J = 8.4 Hz, 1H, CH_{arom}), 9.08 (d, J = 7.4 Hz, 1H, CH_{arom}). MS (DUIS): m/z = 392 [M^+], expected: 392 [M^+]. IR (neat): ῡ (cm^{-1}) = 1765, 1663, 1646, 1577, 1446, 1223, 1228, 1183, 757.

3. Results and Discussion

3.1. Synthesis of 2-Acetoxy-1,4-naphthoquinone

2-Acetoxy-1,4-naphthoquinone (**1**) was prepared from 2-hydroxy-1,4-naphthoquinone in a yield of 80% following a procedure by Clark [34]. The synthesis is described in detail in the Supplementary Materials.

3.2. Photocycloadditions Under Batch Conditions

All batch irradiations followed a modified procedure by Maruyama et al. [36]. Experiments were conducted in Pyrex vessels inside a chamber reactor equipped with fluorescent tubes. Excess amounts of alkene or alkyne were used to prevent photodimerization of **1** [37]. The reaction mixture was constantly purged with a stream of N_2 to remove air and provide mixing.

3.2.1. Optimization Studies

The photoaddition of 1,1-diphenylethylene (**2a**) was initially chosen as a model reaction for process optimization (Scheme 2). A series of exposures for 20 h with different light was subsequently performed in acetone or acetonitrile (Table 1). In line with previous studies [28–30], the reaction chemoselectively produced the cyclobutane adduct **3a** under all experimental conditions, while the formation of spiro-oxetanes was not observed.

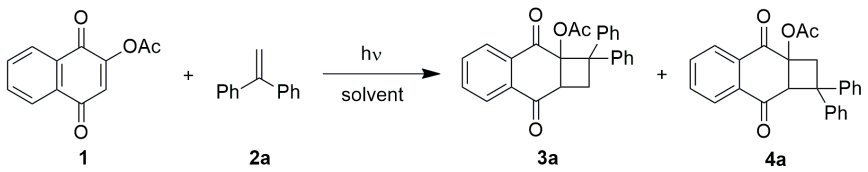

Scheme 2. [2+2]-Photocycloaddition of 2-acetoxy-1,4-naphthoquinone with 1,1-diphenylethylene as a model reaction.

Table 1. Experimental results of the optimization study (Pyrex, 20 h).

Entry	Light	Solvent	Conversion (%) [1]	Composition [1]	
				3a (%)	4a (%)
1	306 ± 20 nm	acetone	88	≥95	n.d. [2]
2	306 ± 20 nm	acetonitrile	82	≥95	n.d. [2]
3	352 ± 20 nm	acetone	100	≥95	n.d. [2]
4	352 ± 20 nm	acetonitrile	100	≥95	n.d. [2]
5	419 ± 25 nm	acetone	78	≥95	n.d. [2]

[1] Determined by ^{1}H-NMR analysis (±3%). [2] Not determined.

Despite the exhaustive reaction time, photocycloadditions of the **1**/**2a** pair remained incomplete when irradiated in either acetone or acetonitrile with UVB or visible light (entries 1, 2 and 5). In contrast, naphthoquinone **1** was completed consumed in both solvents when UVA light was chosen (entries 3 and 4). The absorption spectrum of 2-acetoxy-1,4-naphthoquinone (**1**) has been previously described and shows a dominant and broad benzenoid transition around 335 nm [38–41]. A low intensity but masked quinonoid transition has also been suggested in the 330–450 nm region [40]. These absorptions overlap efficiently with the emission spectrum of the UVA lamp, thus enabling effective excitation (see Supplementary Materials). The electron-donating acetoxy group furthermore increases the energy of the n,π* triplet state of **1** above that of its corresponding π,π* counterpart, hence favoring the addition of the alkene at the quinonoid C=C site [10]. The remarkable *head-to-head* regioselectivity can be explained via a stepwise triplet state mechanism featuring the more stable 1,4-diradical intermediate [42]. For the irradiation in acetone with UVB light (entry 1), competing absorption by the solvent ($T_{10\%}$ = 329 nm [43]) and subsequent triplet sensitization cannot be ruled out [44]. In contrast, direct absorption operates with UVA or visible light in this solvent instead (entries 3 and 5).

3.2.2. Preparative Photocycloadditions with Selected Alkenes

Due to its low toxicity [45], photoprotective nature [24], excellent solvation ability, and easy removability, the photocycloaddition of **1** was subsequently conducted in acetone with selected alkenes (**2a–c**) and utilizing UVA light (Scheme 3). After extended reaction times of 10–20 h, the conversion rates of **1** reached 76–100%. The need to remove unreacted **1** or other minor impurities by automated chromatography reduced isolated yields of the corresponding cyclobutanes **3a–c** to 41–69% (Table 2) [46].

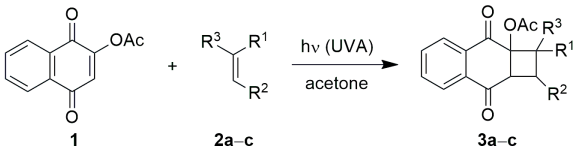

Scheme 3. [2+2]-Photocycloadditions of 2-acetoxy-1,4-naphthoquinone with selected alkenes.

Table 2. Experimental results of selected alkenes (Pyrex, UVA/352 ± 20 nm).

Entry	Alkene (2)			Time (h)	Conversion (%) [1]	Yield (%) [2]
	R^1	R^2	R^3			
1	Ph	H	Ph	20	100	60 (**3a**)
2	Ph	H	H	10	95	69 (**3b**)
3	-$(CH_2)_3$-		H	12	76	41 (**3c**)

[1] Determined by ^{1}H-NMR analysis (±3%). [2] After automated flash chromatography.

Photocycloadditions of **1** with 1,1-diphenylethylene (**2a**) and styrene (**2b**) with artificial light have been previously described [28,29]. While similar isolated yields of approx. 50%

have been achieved for both reactions, the reported procedure used acetonitrile as reaction medium, and a Pyrex immersion-well reactor equipped with a 125 W medium-pressure mercury lamp as the light source. The developed protocol in this study utilized non-hazardous and volatile acetone in combination with more selective UVA light emitted from low heat-generating fluorescent tubes instead.

Photocycloaddition with 1,1-Diphenylethylene

The reaction between 2-acetoxy-1,4-naphthoquinone (**1**) and 1,1-diphenylethylene (**2a**) demanded 20 h for completion and furnished cyclobutane **3a** in an isolated yield of 60% (entry 1). The *head-to-head* structure of **3a** was unambiguously confirmed by X-ray crystallographic analysis (Figure 1). The slightly puckered structure of the cyclobutane system resulted in bond angles in the range of 90–92°, except for the carbon carrying the phenyl substituents, which gave a bond angle of 87° instead [47,48]. The two hydrogen atoms H^3 and H^{10b} were placed at pseudo-equatorial positions, while H^3 and H^{10a} adopted a not quite eclipsed conformation with a dihedral angle of *ca* 14°.

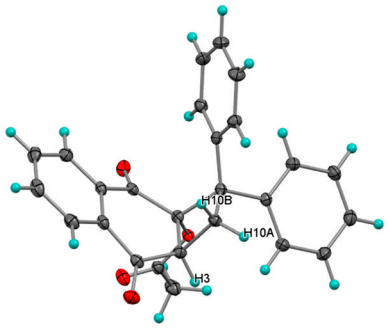

Figure 1. Crystal structure of **3a** (dark grey: carbon, light blue: hydrogen, red: oxygen).

The ^{1}H-NMR spectrum of cycloadduct **3a** in $CDCl_3$ (see Supplementary Materials) showed a sharp singlet at 2.08 ppm for the acetoxy group. The three protons of the cyclobutane system displayed signals between 3.10–4.63 ppm. A pair of doublets at 3.40 and 3.59 ppm with a germinal coupling of ^2J = 12.3 Hz was observed for the methylene protons H^{10a} and H^{10b}, whereas a multiplet at 3.57 ppm represented the remaining proton H^3. The aromatic protons appeared between 6.86 and 7.94 ppm.

Photocycloaddition with Styrene

The photoaddition of styrene **2b** resulted in a conversion of 95% after just 10 h of irradiation. Subsequent automated chromatography produced pure *anti*-**3b** in an isolated yield of 69% (entry 2). X-ray structure analysis confirmed the formation of the *head-to-head* and *anti*-isomer of **3b** (Figure 2). The cyclobutane ring showed a slightly puckered geometry, with bond angles found at 88–91° [47,48]. The shallow ring conformation led to a near eclipsed alignment of H^7 and H^{8A} with a torsion angle of around 17°.

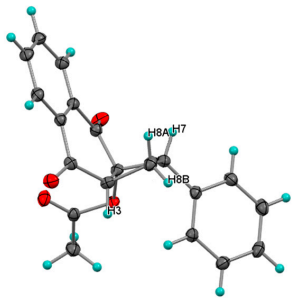

Figure 2. Crystal structure of *anti*-**3b** (dark grey: carbon, light blue: hydrogen, red: oxygen).

The ^{1}H-NMR spectrum of *anti*-**3b** in $CDCl_3$ (see Supplementary Materials) showed the four protons of the cyclobutane ring as four separate signals, i.e., three doublets of doublets at 2.59, 3.11, and 3.62 ppm and one doublet of doublet at 3.98 ppm, respectively. A sharp singlet at 2.00 ppm represented the methyl protons of the acetoxy group. Five separate signals were observed for the aromatic protons, two multiplets between 7.28 and 7.39 ppm (phenyl protons) and three doublets of doublets at 7.84, 8.21 and 8.28 ppm, respectively.

Photocycloaddition with Cyclopentene

Photoirradiation of **1** with cyclopentene (**2c**) for 12 h furnished an incomplete conversion of 76% and solely gave the *anti*-isomer of **3c** in an isolated yield of 41% (entry 3). The crystal structure of *anti*-**3c** is depicted in Figure 3. The structure contained two different cycloalkane conformations. The puckered cyclobutane ring remained rather shallow with bond angles of 89–90° [47,48]. The *cis*-protons H^9 and H^{10} appeared not to be completely eclipsed with a torsion angle of about 6°. The cyclopentane conformation was similar to that found in the corresponding photoadduct with 1,4-naphthoquinone [24].

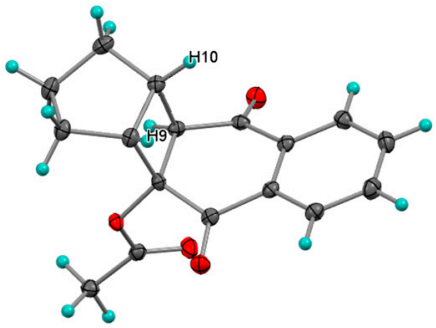

Figure 3. Crystal structure of *anti*-**3c** (dark grey: carbon, light blue: hydrogen, red: oxygen).

In the ^{1}H-NMR spectrum of *anti*-**3c** in $CDCl_3$ (see Supplementary Materials), the six bridging -CH_2- protons of the cyclopentane ring appeared as broad signals at 2.38 and between 1.55 and 1.95 ppm, respectively. A clear singlet at 2.11 ppm represented the acetoxy group. The protons of the cyclobutane moiety gave three signals, which appeared as doublets of doublets at 2.70 and 2.91 ppm and as a doublet at 3.03 ppm, respectively. A set of three multiplets at 7.78, 8.10 and 8.17 ppm represented the four aromatic protons.

3.2.3. Photocycloadditions with Diphenylacetylene

The photoaddition of **1** was furthermore investigated with diphenylacetylene (**5**). Irradiation in acetone for 10 h with UVA light produced cyclobutene **6** and benzoanthracenone **7** in isolated yields of 15 and 9% (Scheme 4), respectively.

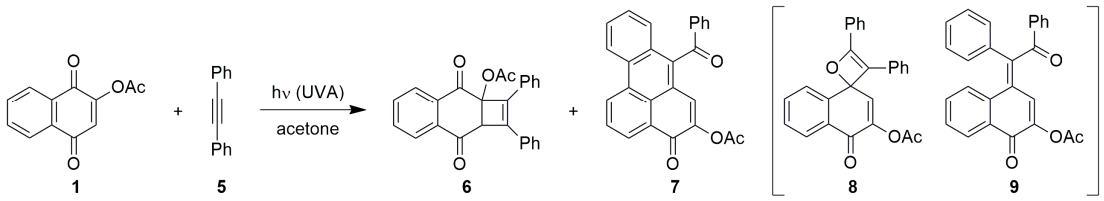

Scheme 4. [2+2]-Photocycloaddition of 2-acetoxy-1,4-naphthoquinone with diphenylacetylene.

Competing photoinduced electron transfer and direct excitation mechanisms have been proposed for the photoaddition involving alkynes [49]. The formation of **7** may be rationalized via ring-opening of the initial *spiro*-oxetene **8** to quinone methide **9**, followed by successive oxidative photodehydrocyclization [49,50]. The reaction has been described by Pappas et al. [35], who isolated compounds **6** and **9** in yields of 20% each after prolonged

irradiation in acetonitrile with UVA light for 31 h. However, the authors did not define the position of the acetoxy group in compound **9**.

The structure of photoadduct **6** was confirmed by X-ray crystallographic analysis (Figure 4). The almost planar structure of the cyclobutene system with a C=C bond length of 1.36 Å resulted in bond angles of 85–95°. The two phenyl groups were placed nearly eclipsed with a dihedral angle of just *ca* 7°.

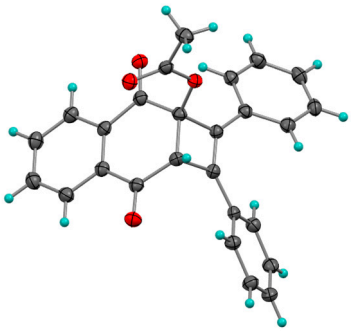

Figure 4. Crystal structure of **6** (dark grey: carbon, light blue: hydrogen, red: oxygen).

The ^{1}H-NMR spectrum of **6** in $CDCl_3$ (see Supplementary Materials) showed five multiplets for the aromatic protons between 7.34 and 8.12 ppm. The single cyclobutene proton showed a singlet at 4.34 ppm [51], while a sharp singlet at 2.22 ppm was observed for the acetoxy group. The structure of the benzoanthracenone **7** was likewise supported by ^{1}H-NMR analysis (see Supplementary Materials). In $CDCl_3$, a total of nine signals with a combined integration of twelve protons were found in the aromatic region. Of these, anisotropy effects shifted the inner aromatic protons of the phenanthrene moiety downfield to 8.80 and 9.08 ppm, respectively [52]. The position of the acetoxy group was assigned by comparison with analog photoadditions involving 2-substituted quinones [49,50,53]. The =CH proton was detected as a singlet at 7.35 ppm, while the acetoxy protons appeared as a strong singlet at 2.32 ppm.

3.3. Photocycloadditions with Selected Alkenes Under Continuous-Flow Conditions

As a proof-of-concept, 2-acetyloxy-1,4-naphthoquinone (**1**) was furthermore reacted with alkenes **3a–c** in an in-house continuous-flow reactor (Scheme 3). Flow rates and hence residence times were varied significantly between experiments to determine the consumption of **1** by ^{1}H-NMR analysis (Table 3).

Table 3. Experimental results of photocyclizations with selected alkenes under continuous-flow conditions (Pyrex, UVA/352 ± 20 nm, acetone).

Entry	Alkene (2)			Residence Time (mins)	Conversion (%) [1]	Yield (%) [2]
	R^1	R^2	R^3			
1	Ph	H	Ph	300	100	55 (**3a**)
2	Ph	H	H	120	97	91 (**3b**)
3	-$(CH_2)_3$-		H	100	36	30 (**3c**)/83 [3]

[1] Determined by ^{1}H-NMR analysis (±3%). [2] After automated flash chromatography. [3] Yield based on consumed **1**.

The general reactivity differences observed in batch were also noted during flow operations, although the latter achieved a significant reduction in irradiation times. However, further residence time optimizations are required to determine realistic productivity rates. 1,1-Diphenylethylene (**2a**) gave complete conversion with a residence time of 300 min, and the cycloadduct **3a** was isolated in a yield of 55% (entry 1). In contrast, styrene (**2a**) reacted readily, showed a near complete conversion of 97% with a residence time of 120 min and

furnished cyclobutane *anti*-**3b** in an excellent yield of 91% (entry 2). The photoaddition of cyclopentene (**2c**) gave the lowest conversion of 36% with the shortest residence time of 100 min. Photoproduct *anti*-**3c** was subsequently obtained in a yield of 30% (or 83% based on consumed **1**). The results from this limited study support previous findings on the general superiority of continuous-flow operations in terms of conversions, yields and irradiation times [17–26]. In particular, the narrow reaction channels allow for effective light penetration, while flow operation removes the potentially photoactive products from the reaction room [17–22]. However, the scale-up, productivity and reproducibility of flow-photochemical processes remain challenging [54–57].

4. Conclusions

In summary, photocycloadditions of 2-acetoxy-1,4-naphthoquinone with selected alkenes and a model alkyne have been successfully realized. The simple irradiation protocol developed uses acetone and UVA light for the construction of cyclobutane and cyclobutene photoproducts in yields of 15–69%. The photoaddition of diphenylacetylene additionally produced a benzoanthracenone derivative in 9% yield. A limited continuous-flow study conducted with the chosen alkenes gave the corresponding photoproducts in similar or improved yields up to 91% but with significantly shorter irradiation times.

Supplementary Materials: The following supporting information can be downloaded at https://www.mdpi.com/article/10.3390/photochem5040031/s1: Technical details, experimental procedure for the synthesis of **1**, crystallographic data and NMR spectra. Figure S1. Rayonet chamber reactor during irradiation. Figure S2. In-house continuous-flow capillary reactor during operation. Figure S3. UV-Vis spectra of **1** (in MeCN) and acetone vs. emissions of UVB, UVA and 419 nm lamps. Table S1. Crystal data and structural refinement for compounds **3a**, *anti*-**3b**, *anti*-**3c** and **6** [58–61].

Author Contributions: M.A.Y., Z.G. and M.O. conducted the research and collected the data; P.C.J. supervised and assisted with the structure determination; M.O. also secured the funding, supervised the chemical research and wrote the manuscript. All authors have read and agreed to the published version of the manuscript.

Funding: This research was funded by the College of Science and Engineering at James Cook University through a Competitive Research Training Grant.

Data Availability Statement: The original contributions presented in this study are included in the article/Supplementary Material. Further inquiries can be directed to the corresponding author.

Acknowledgments: M.A.Y. thanks the Ministry of Higher Education and Scientific Research of Iraq for a Ph.D. Scholarship. Parts of this research was undertaken on the MX1 beamline at the Australian Synchrotron, part of ANSTO.

Conflicts of Interest: Author M.O. is employed by Hochschule Fresenius gGmbH—University of Applied Sciences. The remaining authors declare that the research was conducted in the absence of any commercial or financial relationships that could be construed as a potential conflict of interest.

References

1. Jha, R.K.; Kumar, S. Direct Functionalization of *para*-Quinones: A Historical Review and New Perspectives. *Eur. J. Org. Chem.* **2024**, *27*, e202400535. [CrossRef]
2. Angulo-Elizari, E.; Henriquez-Figuereo, A.; Morán-Serradilla, C.; Plano, D.; Sanmartín, C. Unlocking the Potential of 1,4-Naphthoquinones: A Comprehensive Review of Their Anticancer Properties. *Eur. J. Med. Chem.* **2024**, *268*, 116249. [CrossRef] [PubMed]
3. Navarro-Tovar, G.; Vega-Rodríguez, S.; de Loera, D.; Leyva, E.; Loredo-Carrillo, S.; López-López, L.I. The Relevance and Insights on 1,4-Naphthoquinones as Antimicrobial and Antitumoral Molecules: A Systematic Review. *Pharmaceuticals* **2023**, *16*, 496. [CrossRef] [PubMed]

4. Mone, N.S.; Bhagwat, S.A.; Sharma, D.; Chaskar, M.; Patil, R.H.; Zamboni, P.; Nawani, N.N.; Satpute, S.K. Naphthoquinones and Their Derivatives: Emerging Trends in Combating Microbial Pathogens. *Coatings* **2021**, *11*, 434. [CrossRef]
5. Ahmadi, E.S.; Tajbakhsh, A.; Iranshahy, M.; Asili, J.; Kretschmer, N.; Shakeri, A.; Sahebkar, A. Naphthoquinone Derivatives Isolated from Plants: Recent Advances in Biological Activity. *Mini-Rev. Med. Chem.* **2020**, *20*, 2019–2035. [CrossRef] [PubMed]
6. Perpète, E.A.; Lambert, C.; Wathelet, V.; Preat, J.; Jacquemin, D. *Ab initio* Studies of the λ_{max} of Naphthoquinones Dyes. *Spectrochim. Acta A* **2007**, *68*, 1326–1333. [CrossRef] [PubMed]
7. Jang, J.; Lee, G.; Cho, E.J. Visible Light Induced Reactions of Quinones. *Bull. Korean Chem. Soc.* **2024**, *45*, 966–976. [CrossRef]
8. de Lucas, N.C.; Ferreira, A.B.B.; Netto-Ferreira, J.C. Fotoquímica de Naftoquinonas. *Rev. Virtual Quim.* **2015**, *7*, 403–463. [CrossRef]
9. Maruyama, K.; Osuka, A. Recent advances in the photochemistry of quinones. In *The Chemistry of Quinonoid Compounds*; Patai, S., Rappaport, Z., Eds.; John Wiley & Sons Ltd.: New York, NY, USA, 1988; Volume 2, Part 1, Chapter 13, pp. 759–878. [CrossRef]
10. Gilbert, A. 1,4-Quinone Cycloaddition Reactions with Alkenes, Alkynes, and Related Compounds. In *CRC Handbook of Organic Photochemistry and Photobiology*, 2nd ed.; Horspool, W.M., Lenci, F., Eds.; CRC Press: Boca Raton, FL, USA, 2004; Chapter 87, pp. 1–12. [CrossRef]
11. Creed, D. 1,4-Quinone Cycloaddition Reactions with Alkene, Alkynes and Related Compounds. In *CRC Handbook of Organic Photochemistry and Photobiology*; Horspool, W.M., Song, P.-S., Eds.; CRC Press: Boca Raton, FL, USA, 1995; Chapter 59, pp. 737–747.
12. Tan, S.-B.; Huang, C.; Chen, X.; Wu, Y.; Zhou, M.; Zhang, C.; Zhang, Y. Small Molecular Inhibitors of miR-1 Identified from Photocycloadducts of Acetylenes with 2-Methoxy-1,4-naphthalenequinone. *Bioorg. Med. Chem.* **2013**, *21*, 6124–6131. [CrossRef]
13. Chen, X.; Huang, C.; Zhang, W.; Wu, Y.; Chen, X.; Zhang, C.-Y.; Zhang, Y. A Universal Activator of micro RNAs Identified from Photoreaction Products. *Chem. Comm.* **2012**, *48*, 6432–6434. [CrossRef]
14. Protti, S.; Ravelli, D.; Fagnoni, M. Introduction to Photochemistry for the Synthetic Chemist. In *Enabling Tools and Techniques for Organic Synthesis: A Practical Guide to Experimentation, Automation, and Computation*; Newman, S.G., Ed.; John Wiley & Sons Ltd.: New York, NY, USA, 2023; Chapter 2, pp. 37–72. [CrossRef]
15. Douglas, P.; Evans, R.C.; Burrows, H.D. The Photochemical Laboratory. In *Applied Photochemistry*; Evans, R.C., Douglas, P., Burrows, H.D., Eds.; Springer: Dordrecht, The Netherlands, 2013; Chapter 14, pp. 467–531. [CrossRef]
16. Bochet, C.G. On the Sustainability of Photochemical Reactions. *Chimia* **2019**, *73*, 720–723. [CrossRef] [PubMed]
17. Crawford, R.; Baumann, M. Continuous Flow Technology Enabling Photochemistry. *Adv. Synth. Catal.* **2025**, *367*, e202500133. [CrossRef]
18. Srivastava, V.; Singh, P.P.; Sinha, S.; Singh, P.K.; Kumar, D. Continuous-Flow Photochemistry: The Synthesis of Marketed Pharmaceutical Compounds. *ChemistrySelect* **2024**, *9*, e202405020. [CrossRef]
19. Zhang, M.; Roth, P. Flow photochemistry–From Microreactors to Large-scale Processing. *Curr. Opin. Chem. Eng.* **2023**, *39*, 100897. [CrossRef]
20. Fukuyama, T.; Kasakado, T.; Hyodo, M.; Ryu, I. Improved Efficiency of Photo-induced Synthetic Reactions Enabled by Advanced Photo Flow Technologies. *Photochem. Photobiol. Sci.* **2022**, *21*, 761–775. [CrossRef]
21. Rehm, T.H. Flow Photochemistry as a Tool in Organic Synthesis. *Chem. Eur. J.* **2020**, *26*, 16952–16974. [CrossRef]
22. Oelgemöller, M.; Hoffmann, N.; Shvydkiv, O. From 'Lab & Light on a Chip' to Parallel Microflow Photochemistry. *Austr. J. Chem.* **2014**, *67*, 337–342. [CrossRef]
23. Yaseen, M.A.; Oelgemöller, M. Photochemical Acylation of 1,4-Naphthoquinone with Aldehydes Under Continuous-Flow Conditions. *Organics* **2025**, *6*, 9. [CrossRef]
24. Yaseen, M.A.; Guo, Z.; Junk, P.J.; Oelgemöller, M. [2+2]-Photocycloadditions of 1,4-Naphthoquinone Under Batch and Continuous-Flow Conditions. *Molecules* **2024**, *29*, 5920. [CrossRef]
25. Khan, H.; Rajesh, V.M.; Ravva, M.K.; Sen, S. Optimization of Blue LED Photo-Flow Synthesis in Continuous Flow Reactors Using Design of Experiments (DoE): Efficient Synthesis of Diverse Diaryl Ketones. *Chem. Eng. J.* **2024**, *501*, 157657. [CrossRef]
26. Yaseen, M.A.; Mumtaz, S.; Hunter, R.L.; Wall, D.; Belluau, V.; Robertson, M.J.; Oelgemöller, M. Continuous-Flow Photochemical Transformations of 1,4-Naphthoquinones and Phthalimides in a Concentrating Solar Trough Reactor. *Austr. J. Chem.* **2020**, *73*, 1149–1157. [CrossRef]
27. Yaseen, M.A. Photochemical Transformations of Quinones under Batch and Continuous–Flow Conditions. Ph.D. Thesis, James Cook University, Townsville, QLD, Australia, 2019.
28. Cleridou, S.; Covell, C.; Gadhia, A.; Gilbert, A.; Kamonnawin, P. Photocycloaddition of Arylethenes to 2-Substituted-1, 4-naphthoquinones and Reactions of the Cyclobutane Adduct Isomers. *J. Chem. Soc. Perkin Trans. 1* **2000**, 1149–1155. [CrossRef]
29. Covell, C.; Gilbert, A.; Richter, C. Sunlight-induced Regio-and Stereo-specific ($2\pi + 2\pi$) Cycloaddition of Arylethenes to 2-Substituted-1, 4-naphthoquinones. *J. Chem. Res. (S)* **1998**, 316–317. [CrossRef]
30. Senboku, H.; Kajizuka, Y.; Kobayashi, K.; Tokuda, M.; Suginome, H. Furan Annelation of 2-Hydroxynaphthoquinone Involving Photochemical Addition and Radical Fragmentation: Exclusion of the Intermediacy of [2+2] Cycloadduct in a One-pot Formation of Furanoquinones by the Regioselective 3+2 Photoaddition of Hydroxyquinones with Alkenes. *Heterocycles* **1997**, *44*, 341–348.

31. Mumtaz, S.; Robertson, M.J.; Oelgemöller, M. Continuous Flow Photochemical and Thermal Multi-step Synthesis of Bioactive 3-Arylmethylene-2,3-dihydro-1H-isoindolin-1-ones. *Molecules* **2019**, *24*, 4527. [CrossRef] [PubMed]
32. Fulmer, G.R.; Miller, A.J.; Sherden, N.H.; Gottlieb, H.E.; Nudelman, A.; Stoltz, B.M.; Bercaw, J.E.; Goldberg, K.I. NMR Chemical Shifts of Trace Impurities: Common Laboratory Solvents, Organics, and Gases in Deuterated Solvents Relevant to the Organometallic Chemist. *Organometallics* **2010**, *29*, 2176–2179. [CrossRef]
33. Cowieson, N.P.; Aragao, D.; Clift, M.; Ericsson, D.J.; Gee, C.; Harrop, S.J.; Mudie, N.; Panjikar, S.; Price, J.R.; Riboldi-Tunnicliffe, A.; et al. MX1: A Bending-magnet Crystallography Beamline Serving both Chemical and Macromolecular Crystallography Communities at the Australian Synchrotron. *J. Synchrotron Radiat.* **2015**, *22*, 187–190. [CrossRef]
34. Clark, N.G. The Fungicidal Activity of Substituted 1, 4-Naphthoquinones. Part II: Alkoxy, Phenoxy and Acyloxy derivatives. *Pesticide Sci.* **1984**, *15*, 235–240. [CrossRef]
35. Pappas, S.; Portnoy, N.A. Substituent Effects on the Photoaddition of Diphenylacetylene to 1, 4-Naphthoquinones. *J. Org. Chem.* **1968**, *33*, 2200–2203. [CrossRef]
36. Maruyama, K.; Otsuki, T.; Takuwa, A.; Kako, S. Photochemical Reaction of 1, 4-Naphthoquinone with Olefins. *Bull. Inst. Chem. Res. Kyoto Univ.* **1972**, *50*, 344–347.
37. Dekker, J.; van Vuuren, P.J.; Venter, D.P. Photodimerization. I. The *syn* and *anti*-Photodimers of 1,4-Naphthoquinone. *J. Org. Chem.* **1968**, *33*, 464–466. [CrossRef]
38. Daglish, C. The Ultraviolet Absorption Spectra of Some Hydroxynaphthalenes. *J. Am. Chem. Soc.* **1950**, *72*, 4859–4864. [CrossRef]
39. Hill, R.R.; Mitchell, G.H. The Ultraviolet and Visible Absorption Spectra of Some Polysubstituted 1,4-Naphthaquinones and 9,10-Anthraquinones. *J. Chem. Soc. B* **1969**, 61–64. [CrossRef]
40. Singh, I.; Ogata, R.T.; Moore, R.E.; Chang, C.W.J.; Scheuer, P.J. Electronic spectra of substituted naphthoquinones. *Tetrahedron* **1968**, *24*, 6053–6073. [CrossRef]
41. Macbeth, A.K.; Price, J.R.; Winzor, F.L. The Colouring Matters of Drosera Whittakeri. Part I. The Absorption Spectra and Colour Reactions of Hydroxy-naphthaquinones. *J. Chem. Soc.* **1935**, 325–333. [CrossRef]
42. Crimmins, M.T.; Reinhold, T.L. Enone Olefin [2+2] Photochemistry Cycloaddition. In *Organic Reactions, Paquette, L.A., Ed.*; John Wiley & Sons, Inc.: New York, NY, USA, 1993; Volume 44, pp. 298–579. [CrossRef]
43. Montalti, M.; Credi, A.; Prodi, L.; Gandolfi, M.T. Solvent Properties. In *Handbook of Photochemistry*, 3rd ed.; CRC Press: Boca Raton, FL, USA, 2006; Chapter 9, pp. 535–559. [CrossRef]
44. Bunce, N.J.; Ridley, J.E.; Zerner, M.C. On the Excited States of p-Quinones and an Interpretation of the Photocycloaddition of p-Quinones to Alkenes. *Theor. Chim. Acta* **1977**, *45*, 283–300. [CrossRef]
45. Capello, C.; Fischer, U.; Hungerbühler, K. What is a Green Solvent? A Comprehensive Framework for the Environmental Assessment of Solvents. *Green Chem.* **2007**, *9*, 927–934. [CrossRef]
46. Wernerova, M.; Hudlicky, T. On the Practical Limits of Determining Isolated Product Yields and Ratios of Stereoisomers: Reflections, Analysis, and Redemption. *Synlett* **2010**, 2701–2707. [CrossRef]
47. Cotton, F.A.; Frenz, B.A. Conformations of Cyclobutane. *Tetrahedron* **1974**, *30*, 1587–1594. [CrossRef]
48. Dragojlovic, V. Conformational Analysis of Cycloalkanes. *ChemTexts* **2015**, *1*, 14. [CrossRef]
49. Bosch, E.; Hubig, S.; Kochi, J. Paterno-Büchi Coupling of (Diaryl) Acetylenes and Quinone via Photoinduced Electron Transfer. *J. Am. Chem. Soc.* **1998**, *120*, 386–395. [CrossRef]
50. Farid, S.; Kothe, W.; Pfundt, G. Competitive Photoadditions of Acetylenes to the C=C and C=O Bonds of p-Quinones. *Tetrahedron Lett.* **1968**, *9*, 4147–4150. [CrossRef]
51. Farid, S.; Kothe, W.; Pfundt, G. NMR-study of Cyclobutene Derivatives. *Tetrahedron Lett.* **1968**, *9*, 4151–4154. [CrossRef]
52. Balo, C.; Fernández, F.; González, C.; Lopez, C. ^{1}H NMR Spectra of Monosubstituted Phenanthrenes. *Spectrochim. Acta* **1994**, *50A*, 937–940. [CrossRef]
53. Fadeev, A.A.; Kotora, M. Catalytic vs. Uncatalyzed [2+2] Photocycloadditions of Quinones with Alkynes. *Org. Biomol. Chem.* **2023**, *21*, 6174–6179. [CrossRef]
54. Donnelly, K.; Baumann, M. Scalability of Photochemical Reactions in Continuous Flow Mode. *J. Flow Chem.* **2021**, *11*, 223–241. [CrossRef]
55. Elliott, L.D.; Knowles, J.P.; Koovits, P.J.; Maskill, K.G.; Ralph, M.J.; Lejeune, G.; Edwards, L.J.; Robinson, R.I.; Clemens, I.R.; Cox, B.; et al. Batch versus Flow Photochemistry: A Revealing Comparison of Yield and Productivity. *Chem. Eur. J.* **2014**, *20*, 15226–15232. [CrossRef]
56. Bonfield, H.E.; Mercer, K.; Diaz-Rodriguez, A.; Cook, G.C.; McKay, B.S.J.; Slade, P.; Taylor, G.M.; Ooi, W.X.; Williams, J.D.; Roberts, J.P.M.; et al. The Right Light: DeNovo Design of a Robust Modular Photochemical Reactor for Optimum Batch and Flow Chemistry. *ChemPhotoChem* **2020**, *4*, 45–51. [CrossRef]
57. Loubière, K.; Oelgemöller, M.; Aillet, T.; Dechy-Cabaret, O.; Prat, L. Continuous-flow Photochemistry: A Need for Chemical Engineering. *Chem. Eng. Process.* **2016**, *104*, 120–132. [CrossRef]

58. McPhillips, T.M.; McPhillips, S.E.; Chiu, H.J.; Cohen, A.E.; Deacon, A.M.; Ellis, P.J.; Garman, E.; Gonzalez, A.; Sauter, N.K.; Phizackerley, R.P.; et al. Blu-Ice and the Distributed Control System: Software for Data Acquisition and Instrument Control at Macromolecular Crystallography Beamlines. *J. Synchrotron Radiat.* **2002**, *9*, 401–406. [CrossRef]
59. Kabsch, W. Automatic Processing of Rotation Diffraction Data from Crystals of Initially Unknown Symmetry and Cell Constants. *J. Appl. Crystallogr.* **1993**, *26*, 795–800. [CrossRef]
60. Sheldrick, G.M. Crystal Structure Refinement with SHELXL. *Acta Cryst.* **2015**, *C71*, 3–8. [CrossRef]
61. Dolomanov, O.V.; Bourhis, L.J.; Gildea, R.J.; Howard, J.A.K.; Puschmann, H. OLEX2: A Complete Structure Solution, Refinement and Analysis Program. *J. Appl. Crystallogr.* **2009**, *42*, 339–341. [CrossRef]